sustainability

MDPI

Article

Water Resources Carrying Capacity in Arid and Semi-Arid Resource-Based Industrial Cities: Dynamic Assessment and Scenario Simulation in Baiyin, China

Songhai Yu [1,2], Heping Shu [1,2], Rui Zhang [1,2,*], Na Li [1,2] and Yaling Sun [3]

[1] College of Water Conservancy and Hydropower Engineering, Gansu Agricultural University, Lanzhou 730070, China
[2] Gansu Provincial Agricultural Smart Water-Saving Technology Innovation Center, Lanzhou 730070, China
[3] Gansu Hydrology and Water Resources Center, Lanzhou 730000, China
* Correspondence: zhr_1029@163.com; Tel.: +86-13919108720

Abstract

Arid and semi-arid resource-based industrial cities often face limited water supply, high water demand, and pollution pressure. Using Baiyin City in northwest China as a case, this study assesses water resources carrying capacity (WRCC) with an integrated analytical approach. The indicator system includes 16 indicators covering water resources, population, economy, and water environment. Combined AHP–entropy weighting is used to determine indicator weights. The cloud model is used for grade classification, and a system dynamics (SD) model is used to compare development scenarios. Historical assessment covers 2014–2023, while scenario simulations cover 2024–2035. Per capita water resources (X1), the water resources development and utilization rate (X5), and COD discharge (X15) receive the highest combined weights, accounting for 37.049% of the total weight. WRCC increased from 0.371 in 2014 to 0.635 in 2023, and the grade improved from Grade IV to Grade II, although the trend fluctuated during 2019–2021. By 2035, simulated WRCC reaches 0.705 under the water-saving scenario, 0.655 under sustainable development, 0.643 under natural development, and 0.596 under economic development. Under the scenario settings used in this study, water saving and pollution control lead to higher WRCC values than economic expansion alone.

Keywords: water resources carrying capacity; system dynamics; cloud model; scenario simulation; resource-based industrial cities; arid and semi-arid regions

Check for updates

Academic Editor: Wen Cheng Liu

Received: 26 August 2026
Revised: 22 October 2026
Accepted: 2 November 2026
Published: 11 November 2026

Copyright: © 2026 by the authors. Licensee MDPI, Basel, Switzerland. This article is an open access article distributed under the terms and conditions of the Creative Commons Attribution (CC BY) license.

1. Introduction

Water resources are essential for population, industrial development, and ecological security. In arid and semi-arid regions, limited water supply and rising demand can restrict regional development [1,2]. Water pollution and ecosystem degradation further reduce available water and increase pressure on both human use and river ecosystems [3]. These problems are especially important in resource-based industrial cities, where mining, smelting, energy, chemical industries, agriculture, and urban development often compete for limited water resources. Water Resources Carrying Capacity (WRCC) describes the ability of available water resources to support socio-economic activities while maintaining ecological needs. It reflects the balance between water supply and demand and can support regional planning and water management [4–6].

WRCC studies generally use three types of methods. The first includes static evaluation methods such as principal component analysis, TOPSIS, fuzzy evaluation, and obstacle

degree models. Xu et al. used improved principal component analysis to examine WRCC changes in the Beijing–Tianjin–Hebei urban agglomeration [7]. Liu and Liu combined TOPSIS and GIS to study spatial and temporal differences in Liaoning Province [8]. Jia et al. used a DPSR–TOPSIS–obstacle degree–Markov framework to assess WRCC and land use change in the Cele–Yutian Oasis [9]. These methods are useful for evaluating carrying status, but they are less suited to describing feedback among population, economy, water use, and pollution.

The second group uses dynamic simulation, especially System Dynamics (SD). SD models can represent feedback among population growth, industrial development, water demand, water supply, and pollution. Sun and Yang applied an SD model to WRCC in Xiong'an New Area [10], while Yang et al. combined AHP and SD simulation in Xi'an [11]. Barati et al. used SD to examine water crisis policies from a water–energy–food–land–climate perspective [12]. Other studies have also used methods such as the water ecological footprint to assess regional WRCC [13]. The third group focuses on uncertainty and grade classification. The cloud model links quantitative values with qualitative grades through expectation, entropy, and hyper-entropy [14]. It has been used with other evaluation methods in water carrying capacity studies [15,16].

These approaches have improved WRCC assessment, but historical evaluation, grade classification, and future scenario comparison are not always examined in the same workflow. This issue is relevant for arid and semi-arid resource-based industrial cities, where natural water limits, industrial and agricultural demand, and pollution pressure need to be considered together. Representative differences among related studies are summarized in Appendix A, Table A1.

Baiyin City in central-eastern Gansu Province provides such a case. It is a resource-based industrial city in the upper reaches of the Yellow River and lies in the transition zone between arid and semi-arid regions [17]. The city has limited water resources, strong evaporation, and high demand from both industry and agriculture. Its economy also includes non-ferrous metal mining, processing, smelting, energy, and chemical industries. At the same time, Baiyin faces the need for pollution control, reclaimed water use, ecological restoration, and industrial transition. These features make it suitable for examining WRCC changes under different development conditions. The study does not assume that Baiyin represents all arid-region cities, but its experience can provide a useful case for similar resource-constrained industrial cities.

This study applies established weighting, cloud-model, and SD methods to WRCC assessment in Baiyin. It addresses three questions: which indicators receive the highest weights in the composite index, how WRCC changed from 2014 to 2023, and how four development scenarios compare from 2024 to 2035. The study links historical assessment, grade classification, and scenario comparison in one analytical workflow. It does not propose a new weighting, cloud-model, or SD method. The future results are treated as exploratory comparisons under the specified model structure and scenario settings.

2. Case Study

2.1. Study Area

Baiyin City is located in central-eastern Gansu Province, China (35°33′–37°38′ N, 103°33′–105°34′ E). It lies at the transition between the Loess Plateau and the Tengger Desert, where the arid zone of northwest China gradually shifts toward a semi-arid environment. Baiyin is also a typical resource-depleted industrial city in the upper reaches of the Yellow River [17] (Figure 1). This location places the city in a specific development context. It is part of both China's Western Development Strategy and the Yellow River ecological protection and high-quality development strategy, and it is an important component of the

Lanzhou–Baiyin urban agglomeration [18]. The study covers the full municipal jurisdiction of Baiyin City and uses municipal-level aggregated statistics. No district-level analysis is conducted. The analysis includes agricultural, industrial, domestic, and ecological water use. The Yellow River is an important part of Baiyin's water-resource context. These conditions make Baiyin a suitable case for examining the links among water scarcity, resource-based industrial development, and ecological governance in arid and semi-arid cities.

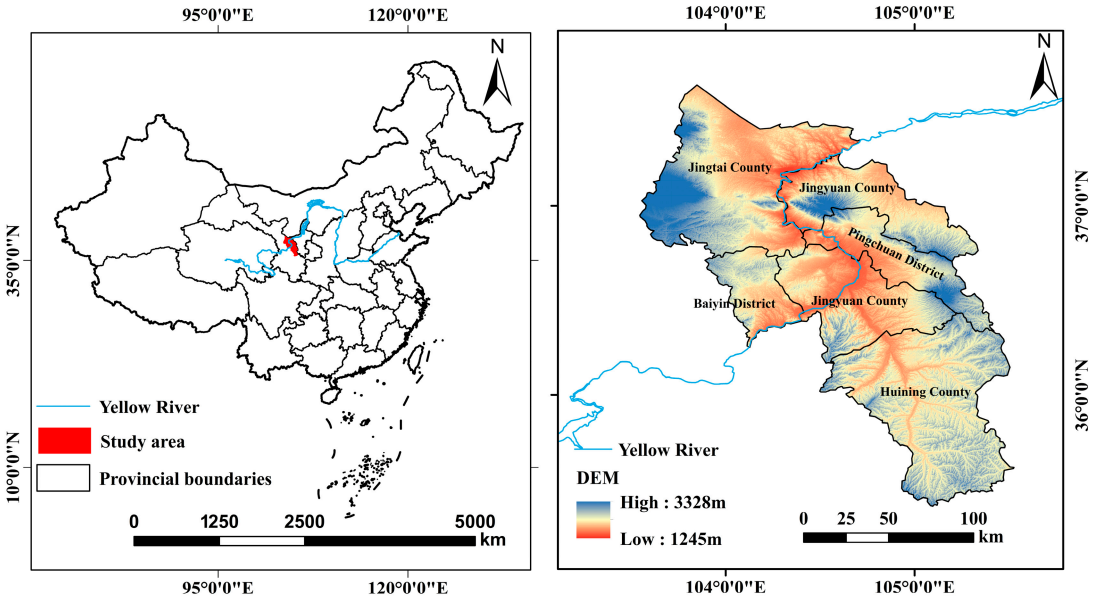


Figure 1. Location and overview of Baiyin City.

The hydroclimatic conditions of Baiyin impose strong limits on water availability. Annual precipitation is generally between 180 and 450 mm, with clear spatial variation, while the multi-year average evaporation reaches 2065.2 mm, nearly ten times the annual precipitation. Per capita water resources in the most recent three-year statistics are only 103.40 m^3, far below the commonly used 500 m^3 threshold for extreme water scarcity. The structure of water use adds further pressure. Average agricultural water use over the same period reached 868 million m^3, compared with 56 million m^3 for domestic use, 64 million m^3 for industrial use, and 21 million m^3 for ecological use. Agriculture remains the dominant water user, while industrial production and urban development continue to increase demand. This water-use structure creates several management challenges, including supply–demand imbalance, low agricultural water-use efficiency, local groundwater overexploitation, ecological degradation, and coordination difficulties between basin-scale water management and urban water withdrawal [19,20].

2.2. Data Sources

The empirical database covers two periods: 2014–2023 for historical WRCC assessment and SD historical fitting, and 2024–2035 for scenario simulation. Data were collected from the Gansu Water Resources Bulletin, Gansu Statistical Yearbook, Baiyin Statistical Yearbook, Baiyin Statistical Bulletin of National Economic and Social Development, ecological and environmental statistics, and relevant government planning documents. These sources were used to construct a consistent database for Water Resources Carrying Capacity (WRCC) assessment and System Dynamics (SD) simulation. All raw data were checked, harmonized, and standardized to ensure consistency between the evaluation indicators and the variables used in the SD model. The dataset was organized according to the structure of the WRCC indicator system and the SD model. The database was organized into four subsystems:

water resources, population, economy, and water environment. The main indicators, data sources, and uses are summarized in Table 1.

Table 1. Data sources and uses for the WRCC assessment and SD simulation.

Subsystem	Main Indicators	Data Sources	Use
Water resources	Total water resources; surface water resources; groundwater resources; total water supply; total water use; per capita water resources; water resources development and utilization rate; water production modulus, etc.	Gansu Water Resources Bulletin; Baiyin Water Resources Bulletin	WRCC assessment; SD model historical fitting and scenario simulation
Population	Permanent population; urban population; urbanization rate; natural population growth rate, etc.	Gansu Statistical Yearbook; Baiyin Statistical Yearbook	WRCC assessment; SD model historical fitting and scenario simulation
Economy	Gross domestic product (GDP); added value of primary, secondary, and tertiary industries; industrial added value; per capita GDP; water use per 10,000 yuan of GDP; water use per 10,000 yuan of industrial added value, etc.	Gansu Statistical Yearbook; Baiyin Statistical Yearbook	WRCC assessment; SD model historical fitting and scenario simulation
Water environment	Ecological water use; wastewater discharge; chemical oxygen demand (COD) discharge; wastewater treatment rate; reclaimed water use; environmental protection investment, etc.	Gansu Statistical Yearbook; Gansu Water Resources Bulletin	WRCC assessment; SD model historical fitting and scenario simulation

For indicators reported directly in statistical records, the original values were retained. Derived indicators were calculated from the corresponding basic variables. Per capita water resources were calculated from total water resources and permanent population; water production modulus was calculated from total water resources and regional area; water use per 10,000 yuan of GDP was calculated from total water use and GDP; and water use per 10,000 yuan of industrial added value was calculated from industrial water use and industrial added value.

The archived data were checked for indicator names, year correspondence, units, and consistency between the assessment indicators and SD variables. These checks were used to support the historical assessment and scenario comparison. The archived records do not retain an indicator-year interpolation log, so specific interpolation steps are not reported.

For the SD model, data from 2014 to 2023 were used for model construction and historical fitting, and 2023 was set as the baseline year for scenario simulation. Key parameters, including population growth rate, industrial growth rate, water-use quota, wastewater discharge coefficient, wastewater treatment rate, and reclaimed water utilization rate, were set using historical statistics, regional planning documents, and scenario assumptions. Historical fitting errors were used to describe model performance. Independent hold-out validation and systematic uncertainty analysis were not conducted. The scenario results are therefore treated as relative comparisons under the specified model structure and parameter settings, rather than as deterministic forecasts.

3. Methods

3.1. Methodological Framework

This study applied an integrated analytical workflow using established methods for assessing the Water Resources Carrying Capacity (WRCC) of Baiyin City by combining indicator weighting, cloud model evaluation, and System Dynamics (SD) simulation. The workflow links historical assessment, grade classification, and future scenario comparison within a single analytical process. First, a WRCC indicator system was constructed from four subsystems: water resources, population, economy, and water environment. The indicators were selected to reflect water supply conditions, development and utilization pressure, socio-economic demand, and water environmental governance in an arid and semi-arid resource-based industrial city. Second, indicator weights were determined using a combined weighting approach. The Analytic Hierarchy Process (AHP) was used to reflect subjective judgments made by the research team, the entropy weight method was used to capture data variation, and an improved game theory-based weighting method was used to integrate the two sets of weights. Third, the cloud model was applied to classify WRCC levels, because the boundaries between quantitative WRCC values and qualitative carrying states are not always clear. Finally, an SD model was built in VENSIM (version 7.3.5; Ventana Systems, Inc., Harvard, MA, USA) to simulate the feedback relationships among population growth, industrial development, water demand, water supply, pollution discharge, and water environmental governance. Data from 2014 to 2023 were used for model construction and historical fitting, and 2023 was set as the baseline year for simulating WRCC changes under different development scenarios from 2024 to 2035. The scenario results were used for relative comparison under specified model assumptions, rather than as deterministic forecasts of future policy effects.

3.2. WRCC Indicator System

WRCC is shaped by the interaction of resource conditions, social demand, economic development, and environmental pressure. For arid and semi-arid resource-based industrial cities, carrying capacity is affected not only by water endowment, but also by industrial water use, population concentration, water-use efficiency, pollution discharge, and water recycling capacity. Based on previous WRCC studies, the characteristics of Baiyin City, and data continuity, this study constructed an indicator system with four subsystems and 16 indicators [21–23]. The water resources subsystem represents the physical supply basis and development pressure of regional water resources. The population subsystem reflects population concentration and domestic water demand. The economy subsystem captures economic development and water-use efficiency. The water environment subsystem describes ecological water allocation, ecological water consumption intensity, pollution pressure, and reclaimed water utilization. Table 2 presents the WRCC assessment indicator system for Baiyin City. Positive indicators indicate that higher values contribute to higher WRCC, while negative indicators indicate that higher values reduce WRCC. All indicators were standardized according to their attributes before the comprehensive assessment, so that indicators with different units and directions could be compared within the same evaluation framework.

Ecological water consumption intensity (X13) was treated as a positive indicator under the final assessment criteria. Pearson correlations were examined for 16 indicators using 10 annual observations from 2014–2023. The analysis identified 56 pairs with $|r| \geq 0.70$, showing strong correlations and a possible risk of double counting. Statistical correlation does not necessarily mean conceptual duplication. The indicators represent resource availability, water-use intensity, economic efficiency, and environmental pressure, so they were retained.

With only 10 observations for 16 indicators, PCA or factor analysis would not provide a stable basis for dimensional reduction. The full matrix is reported in Appendix A, Table A2.

Table 2. WRCC assessment indicator system for Baiyin City.

Objective	Subsystem	Indicator	Unit	Calculation or Data Source	Interpretation	Attribute
Water Resources Carrying Capacity	Water resources	Per capita water resources (X1)	m^3	Total water resources/total population	Per capita water availability	Positive
		Water production modulus (X2)	$10^4m^3/km^2$	Total water resources/regional area	Water yield per unit area	Positive
		Per capita water supply (X3)	m^3	Total water supply/total population	Per capita water supply level	Positive
		Share of surface water resources (X4)	%	Surface water resources/total water resources	Surface water availability within total water resources	Positive
		Water resources development and utilization rate (X5)	%	Total water supply/total water resources	Intensity of water resources development and utilization	Negative
	Population	Population density (X6)	persons/km^2	Total population/regional area	Population pressure per unit area	Negative
		Urbanization rate (X7)	%	Urban population/total population	Level of urbanization	Positive
		Per capita domestic water use (X8)	L/person·day	Domestic water use/total population	Intensity of domestic water use	Negative
	Economy	Per capita GDP (X9)	yuan	GDP/total population	Per capita economic development level	Positive
		Water use per 10,000 yuan of GDP (X10)	m^3	Total water use/GDP	Water consumption intensity of economic output	Negative
		Water use per 10,000 yuan of industrial added value (X11)	m^3	Industrial water use/industrial added value	Industrial water-use intensity	Negative

Table 2. *Cont.*

Objective	Subsystem	Indicator	Unit	Calculation or Data Source	Interpretation	Attribute
Water Resources Carrying Capacity	Water environment	Ecological water allocation rate (X12)	%	Ecological water use/total water use	Share of water allocated to ecological purposes	Positive
		Ecological water consumption intensity (X13)	%	Gansu Water Resources Bulletin	Ecological water consumption level	Positive
		Wastewater discharge (X14)	10^8 m^3	Gansu Water Resources Bulletin	Wastewater discharge pressure	Negative
		Chemical oxygen demand (COD) discharge (X15)	10^4 t	Gansu Statistical Yearbook	Organic pollution load in water bodies	Negative
		Treated wastewater reuse (X16)	m^3	Gansu Water Resources Bulletin	Water recycling and reuse capacity	Positive

3.3. Indicator Standardization and Combined Weighting

The WRCC indicators differ in units, value ranges, and directional attributes. The raw indicators were therefore standardized before evaluation. For positive indicators, higher values indicate a stronger contribution to WRCC. For negative indicators, higher values indicate a weaker contribution to WRCC. After standardization, all indicators were converted into comparable values, and larger standardized values represented more favorable conditions for WRCC. The min–max normalization method was applied to eliminate dimensional differences among indicators.

For positive indicators:

$$z_{ij} = \frac{X_{ij} - X_j^{\min}}{X_j^{\max} - X_j^{\min}} \quad (1)$$

For negative indicators:

$$z_{ij} = \frac{X_j^{\max} - X_{ij}}{X_j^{\max} - X_j^{\min}} \quad (2)$$

where X_{ij} is the original value of indicator j in year i, z_{ij} is the standardized value, and $X_j^{\max}$ and $X_j^{\min}$ are the upper and lower reference values of indicator j used in the archived standardization procedure. After standardization, all indicators were converted into comparable values, and larger standardized values represented more favorable conditions for WRCC. This step provided a common basis for weight integration and WRCC calculation.

The historical WRCC scores were checked against the stored evaluation inputs and combined weights. A separate weighted calculation agreed with the reported three-decimal scores for nine of the ten historical years. The comparison does not establish that the same normalization bounds were used across all future scenarios. The scenario results are therefore interpreted within the evaluation settings used in this study.

AHP was used for the subjective weighting component based on judgments made by the research team. Pairwise judgments were constructed by the research team with reference to the indicator framework and the existing WRCC literature. This component reflects the structure of the indicator system and informed judgment [24,25]. The entropy

weight method represents variation in the historical data [26–28]. The improved game theory method was then used to combine the subjective AHP weights and the data-driven entropy weights. The available AHP, entropy, and combined weights are retained. The three weighting schemes were also compared using the same stored historical evaluation inputs. This comparison examines how the choice of weights affects the WRCC scores and grades. It does not serve as a consistency test for the AHP pairwise judgments.

Assume that p single weighting methods are used. Let ω_k denote the weight vector obtained from the k − th method, and let α_k denote its combination coefficient. The combined weight vector ω^* is expressed as:

$$\omega^* = \sum_{k=1}^{p} \alpha_k \omega_k^T \tag{3}$$

where ω^* is the final combined weight vector, ω_k is the weight vector obtained from the k − th single weighting method, and α_k is the corresponding combination coefficient.

The improved game theory-based weighting method seeks a combined solution that minimizes the deviation among different single-weighting results. To avoid negative combination coefficients, a non-negative constraint was introduced into the optimization process. The model is written as:

$$\begin{cases} \min F = \sum_{s=1}^{p} \left(\sum_{k=1}^{p} \alpha_k \omega_s \omega_k^T - \omega_s \omega_s^T \right)^2 \\ \text{s.t.} \sum_{k=1}^{p} \alpha_k^2 = 1, \alpha_k > 0 \end{cases} \tag{4}$$

where ω_s is the weight vector obtained from the s − th single weighting method. The formulation in Equations (3) and (4) describes the combination of the weighting components. It integrates subjective AHP weights and data-driven entropy weights [29–33].

The combination coefficients were reconstructed from the archived weight vectors. The reconstructed AHP coefficient was approximately 0.5716 and the entropy coefficient was 0.4284. These coefficients reproduced the archived combined weights with only negligible numerical differences. The maximum absolute reproduction error was below 0.000007. These are reconstructed values, not the original recorded optimization coefficients.

After the combined weights were obtained, the annual WRCC value was calculated using the standardized indicators:

$$\text{WRCC}_i = \sum\nolimits_{j=1}^{m} \omega_j^* z_{ij} \tag{5}$$

where WRCC_i is the comprehensive WRCC value in year i, ω_j^* is the combined weight of indicator j, z_{ij} is the standardized value of indicator j in year i, and m is the number of indicators. The calculated WRCC values were then used as the basis for cloud model-based grade classification and historical carrying status analysis.

To examine the effect of weighting, the historical evaluation inputs were assessed using the AHP, entropy, and combined weights. All three methods showed an increase in WRCC between 2014 and 2023, although some grades differed. The yearly results are provided in Appendix A, Table A7.

3.4. Cloud Model-Based WRCC Assessment

The cloud model was used as an auxiliary grade-classification procedure for annual WRCC. The five grade intervals are analytical classification intervals adopted in this study, not official regulatory thresholds (Table 3). Because the boundaries between adjacent grades are not always clear, the cloud model was used to represent the fuzziness and randomness in converting quantitative values into qualitative grades. Each grade cloud is described by three numerical parameters: expectation (E_x), entropy (En), and hyper-entropy (He). E_x

represents the central value of a grade, *En* reflects the acceptable value range of that grade, and *He* describes the uncertainty of entropy. Following previous cloud model studies, *He* was set to 0.01 [34].

Table 3. Classification criteria for WRCC grades.

Grade	Carrying Status	Value Range
V	Overloaded	(0, 0.2]
IV	Marginally overloaded	(0.2, 0.4]
III	Acceptable	(0.4, 0.6]
II	Good	(0.6, 0.8]
I	Ideal	(0.8, 1.0]

In a forward cloud generator, a random entropy realization is represented as:

$$En' \sim \mathrm{N}(En, \mathrm{H}e^2) \tag{6}$$

Then, for a WRCC value x, its membership degree in a given grade cloud was calculated as:

$$\mu(x) = \mathrm{e}^{-\frac{(x-E_x)^2}{2E_n'^2}} \tag{7}$$

where x is the WRCC evaluation value, E_x is the expectation of the corresponding grade cloud, and E_n' is the random entropy realization. $\mu(x)$ represents the membership degree of the WRCC value to the corresponding grade cloud.

To reduce the uncertainty caused by grade boundaries, the improved optimal entropy algorithm was used. This algorithm minimizes the deviation between membership degrees calculated under different entropy rules, including the "3σ" rule (En) and the "50% association degree" rule [35,36]. The deviation is expressed as:

$$\Delta\mu_{\max_i} = \left(\mu_{\max_i} - \mu_{\exp_i}\right)^2 + \left(\mu_{\exp_i} - \mu_{\min_i}\right)^2 \tag{8}$$

where $\mu_{\max_i}$, $\mu_{\min_i}$, and $\mu_{\exp_i}$ are the membership degrees calculated using the upper-bound entropy, lower-bound entropy, and optimized entropy for grade i, respectively. This equation describes the entropy-based classification process. The comparison reported in Table A3 focuses on the final assigned grades. It does not assess variations in membership values across repeated stochastic runs. The reported cloud-model classifications and fixed-threshold classifications agreed in all ten historical years, with an agreement rate of 100% (Appendix A, Table A3).

3.5. SD Model Construction and Historical Fitting

The System Dynamics (SD) model was used to describe the dynamic feedback among population, economy, water resources, and water environment in the WRCC system. In water resource studies, SD models are useful because they can represent stock accumulation, flow changes, and feedback regulation within one system structure [37]. The general stock equation is expressed as:

$$L(t) = L(0) + \int_0^t [R_{\mathrm{in}}(\tau) - R_{\mathrm{out}}(\tau)]d\tau \tag{9}$$

where $L(t)$ is the value of the stock variable at time t, $L(0)$ is the initial value, $R_{in}(\tau)$ is the inflow rate, and $R_{out}(\tau)$ is the outflow rate.

Based on the structure of Baiyin's WRCC system, an SD model was built in VENSIM. The model includes four subsystems: water resources, population, economy, and water environment. Historical data from 2014 to 2023 were used to assess the model's historical fit. The model was applied to scenario simulation for 2024–2035. The main parameters

include population growth rate, industrial growth rate, water-use quota, water supply capacity, wastewater treatment rate, reclaimed water utilization rate, and pollution discharge coefficient. These parameters were used to represent the links between socio-economic development and resource and environmental constraints [38].

The water resources subsystem represents the physical supply basis of the WRCC system. It links total water supply, sectoral water demand, and the water balance coefficient [39]. Total water supply includes surface water, groundwater, and available water supply capacity, while total water demand includes agricultural, industrial, domestic, and ecological water use [40]. Population growth and economic expansion increase water demand, while water-saving measures and higher water-use efficiency can reduce water pressure [41] (Figure 2). The water balance coefficient was calculated as:

$$W_b = \frac{W_s}{W_d} \tag{10}$$

where W_b is the water balance coefficient, W_s is total water supply, and W_d is total water demand. A lower W_b indicates a higher level of water resource pressure and a weaker carrying capacity [42].

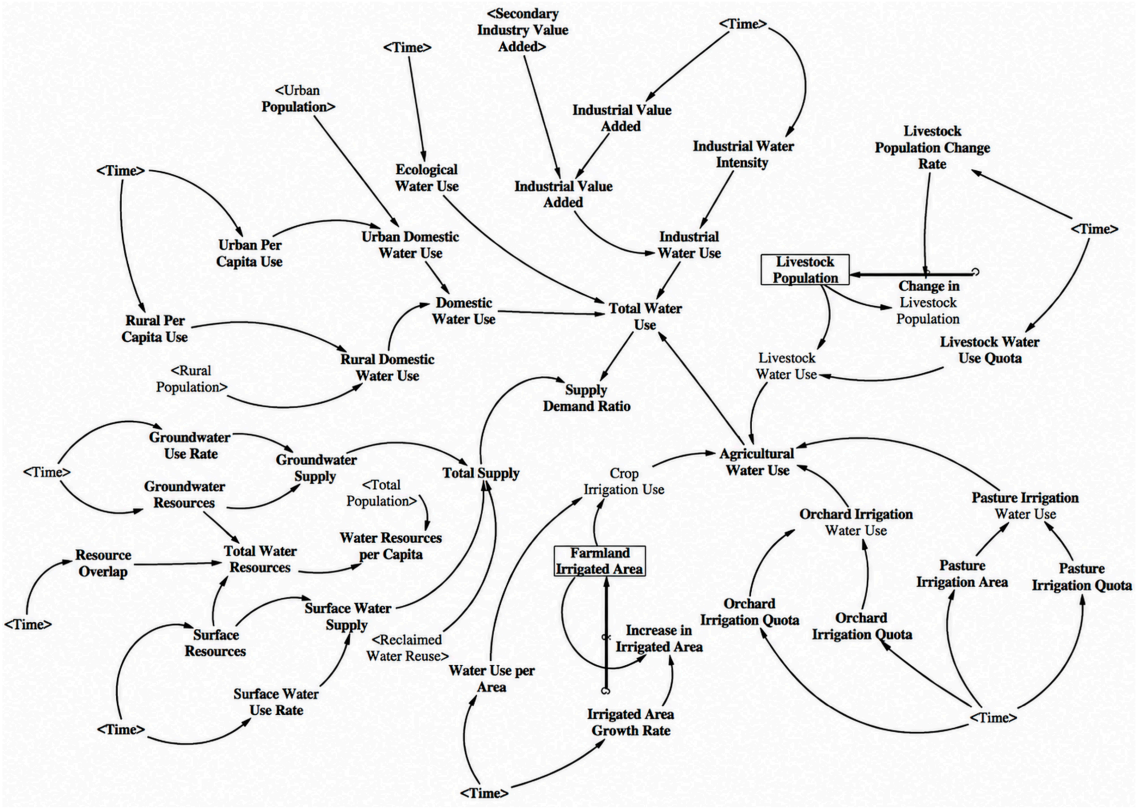


Figure 2. Dynamic structure of the water resources subsystem.

The population subsystem describes changes in population size, urbanization, and domestic water demand. Population growth affects domestic water use and wastewater generation, and it also influences the economy through labor supply, consumption demand, and urbanization [43]. In the model, population-related variables link social demand with water consumption and pollutant discharge. This subsystem therefore affects WRCC through both water demand and water environment pressure [44] (Figure 3).

The economy subsystem represents the scale and structure of regional economic development. GDP and the added value of primary, secondary, and tertiary industries are the main variables in this subsystem [45]. Different industries have different water-use

intensities, so changes in industrial structure affect total water demand and water-use efficiency [46]. Economic growth can increase water consumption and pollution discharge, but it can also support water-saving technologies, environmental investment, and improved resource management. The economy subsystem can therefore place pressure on WRCC while also supporting its improvement [47] (Figure 4).

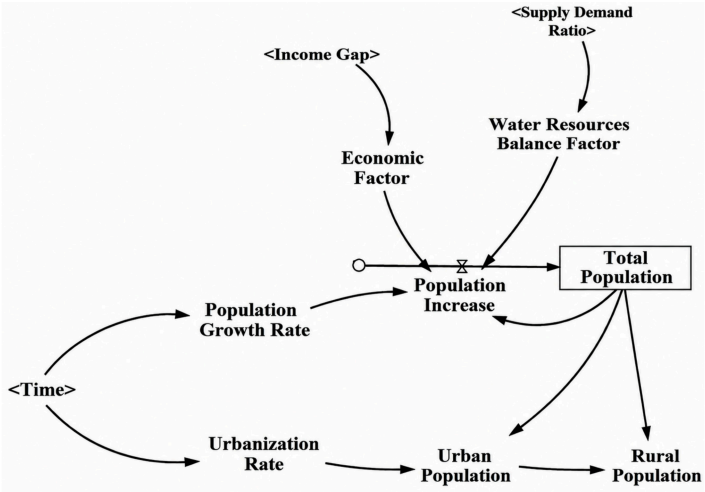


Figure 3. Dynamic structure of the population subsystem.

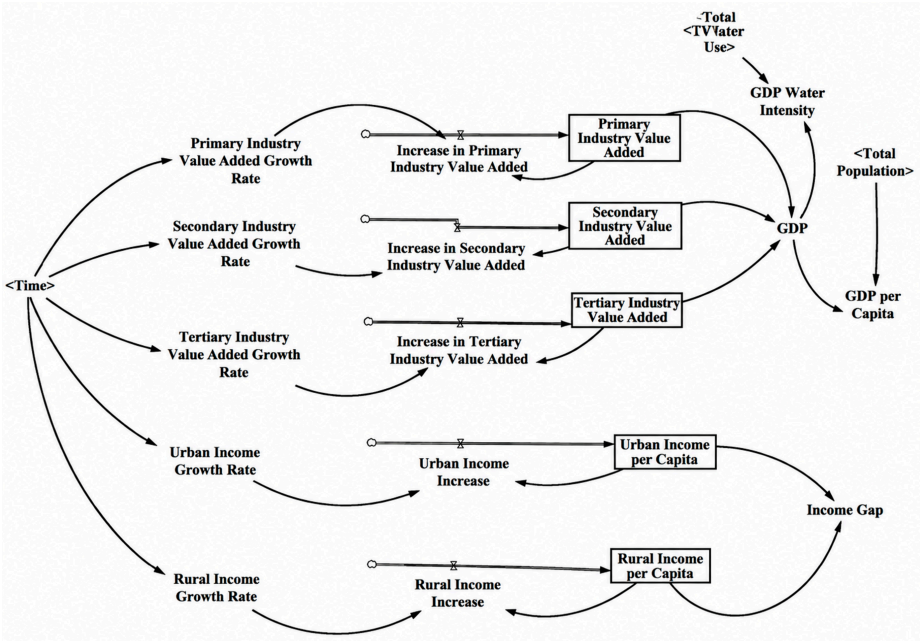


Figure 4. Dynamic structure of the economy subsystem.

The water environment subsystem describes pollution discharge, wastewater treatment, reclaimed water use, and ecological water use. Water environment quality affects the amount and quality of water available for human use and ecosystem functions [3]. Wastewater and COD discharge mainly come from production and domestic activities, while wastewater treatment and reclaimed water use can reduce environmental pressure and improve water recycling capacity [48]. This subsystem connects economic and population activities with water quality and directly affects the environmental dimension of WRCC (Figure 5).

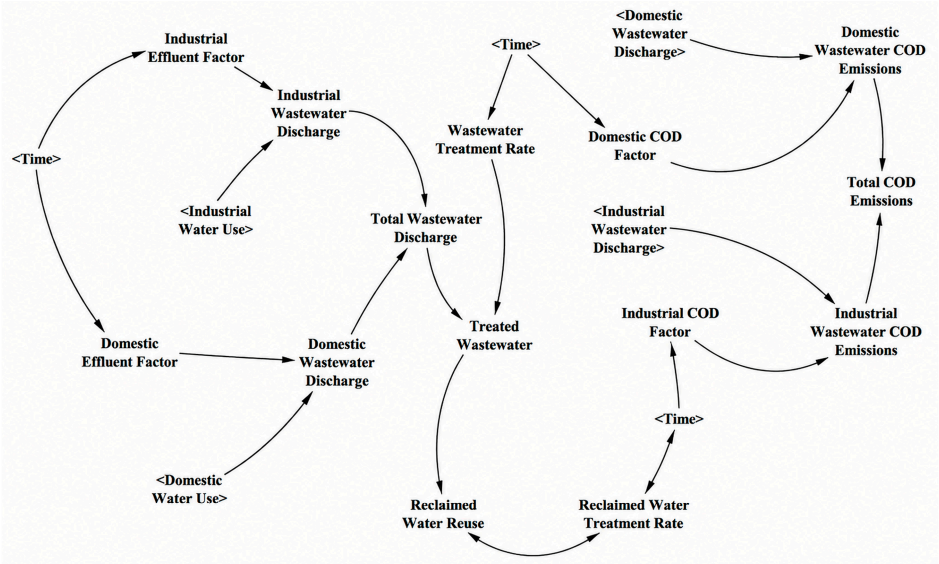


Figure 5. Dynamic structure of the water environment subsystem.

Historical fitting was examined by comparing archived simulated values with historical observations from 2014 to 2023. Six representative variables were selected: total population, GDP, total water use, total water supply, wastewater discharge, and COD discharge. These variables cover the four subsystems. Relative error was calculated as follows [49,50]:

$$E = \frac{S - H}{H} \times 100\% \quad (11)$$

where E is the relative error, S is the simulated value, and H is the historically observed value. MAE, RMSE, MAPE, and R^2 were also used to describe historical fitting. R^2 was calculated as 1 − SSE/SST, not as squared Pearson correlation. These metrics describe in-sample historical fitting and should not be interpreted as evidence of out-of-sample predictive validity. Full metrics and annual errors are reported in Appendix A, Tables A4 and A5. Key equations, parameter definitions, units, and initial values are summarized in Appendix A, Table A6. An equation-level implementation check and a local parameter sensitivity analysis were also conducted. These tests examine the numerical results and parameter responses of the baseline SD model. They do not replace independent out-of-sample validation.

3.6. Scenario Design

Four scenarios were designed to compare WRCC responses under different development assumptions: the natural development scenario, economic development scenario, water-saving scenario, and sustainable development scenario [51,52]. The period from 2014 to 2023 was used for historical simulation, during which all scenarios followed the original model parameters. For the scenario simulation period from 2024 to 2035, key parameters were adjusted relative to the 2023 baseline values, as shown in Table 4. The entries are relative multiplicative adjustments to the corresponding baseline model parameters, not percentage-point changes. Thus, 1.00 means no adjustment, 1.05 means a 5% increase, and 0.94 means a 6% decrease. The baseline population growth rate is negative. For this parameter, a multiplier of 1.05 makes the rate more negative rather than increasing population growth. These scenario settings were defined relative to the 2023 baseline to represent different development paths. They are not documented official policy targets. The natural development scenario assumes that the main parameters continue along the historical trend without additional adjustment. The economic development scenario uses larger adjustment factors for several growth, demand, and discharge parameters. The

water-saving scenario reduces agricultural, industrial, and domestic water-use intensities, and also lowers wastewater and COD discharge coefficients. The sustainable development scenario combines moderate economic growth with stronger water-saving measures, higher wastewater treatment rates, and increased reclaimed water use. For proportional parameters, values greater than 1 after adjustment were capped at 1. The four scenarios were used to compare WRCC responses under different development assumptions. The scenario ranking is conditional on these parameter settings. The results are exploratory comparisons rather than deterministic forecasts of policy outcomes.

Table 4. Scenario settings for the WRCC system dynamics model in Baiyin City.

Parameter	Natural Development Scenario	Economic Development Scenario	Water-Saving Scenario	Sustainable Development Scenario
Population growth rate	1.00	1.05	1.00	1.00
Livestock growth rate	1.00	1.03	1.00	1.00
Livestock water-use quota	1.00	1.03	0.94	0.94
Growth rate of primary industry added value	1.00	1.03	1.00	1.02
Growth rate of secondary industry added value	1.00	1.12	1.00	1.05
Growth rate of tertiary industry added value	1.00	1.10	1.00	1.08
Urban residents' income growth rate	1.00	1.08	1.00	1.05
Rural residents' income growth rate	1.00	1.06	1.00	1.05
Urbanization rate	1.00	1.08	1.00	1.05
Urban per capita domestic water use	1.00	1.05	0.94	0.95
Rural per capita domestic water use	1.00	1.03	0.95	0.96
Water use per 10,000 yuan of industrial added value	1.00	1.08	0.90	0.88
Irrigation water use per unit area	1.00	1.00	0.92	0.90
Orchard irrigation quota	1.00	1.00	0.90	0.90
Grassland irrigation quota	1.00	1.00	0.94	0.92
Surface water development rate	1.00	1.05	1.00	1.03
Groundwater development rate	1.00	1.03	0.97	0.95
Wastewater treatment rate	1.00	1.05	1.08	1.15
Reclaimed water utilization rate	1.00	1.05	1.10	1.15
Domestic wastewater discharge coefficient	1.00	1.05	0.95	0.92
Industrial wastewater discharge coefficient	1.00	1.08	0.92	0.90
Domestic wastewater COD discharge coefficient	1.00	1.05	0.94	0.90

4. Results

4.1. Indicator Weights for WRCC Assessment

The combined weighting results show that per capita water resources (X1) had the largest weight, accounting for 15.564% of the total weight (Figure 6; Table 5). It was followed

by the water resources development and utilization rate (X5, 11.136%) and chemical oxygen demand (COD) discharge (X15, 10.349%). Together, these three indicators accounted for 37.049% of the total weight. These are the highest-weighted indicators within the composite index. Weights indicate relative importance in the constructed index, not real-world causal influence. At the subsystem level, the water resources subsystem contributed a large share of the total weight, showing the importance of natural water availability in this arid and semi-arid setting. Within the water environment subsystem, COD discharge (X15) and wastewater discharge (X14) had relatively high weights, showing that pollution load is also an important part of overall carrying capacity. Differences between the AHP weights and entropy weights were observed for several indicators, including X1, X5, X6, X9, and X16. These differences show that subjective judgment and data variation assigned importance in different ways.

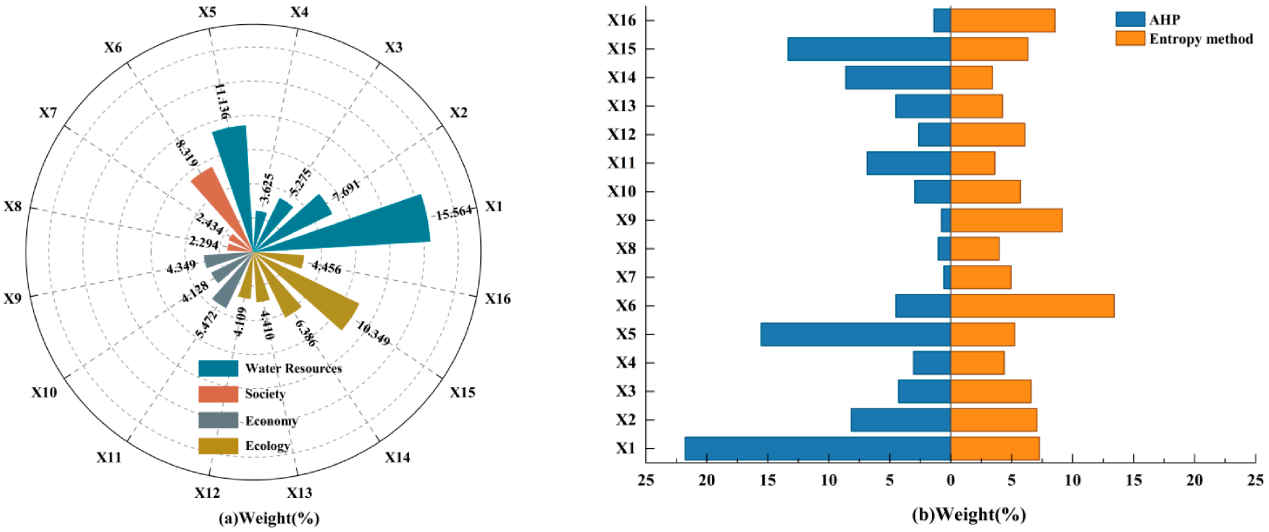


Figure 6. Combined weights of WRCC assessment indicators in Baiyin City.

Table 5. Weights of WRCC assessment indicators in Baiyin City.

Indicator	AHP Weight (%)	Entropy Weight (%)	Combined Weight (%)
X1	21.776	7.276	15.564
X2	8.164	7.060	7.691
X3	4.289	6.592	5.275
X4	3.061	4.378	3.625
X5	15.542	5.257	11.136
X6	4.504	13.411	8.319
X7	0.558	4.936	2.434
X8	1.038	3.971	2.294
X9	0.76	9.137	4.349
X10	2.947	5.704	4.128
X11	6.859	3.622	5.472
X12	2.631	6.082	4.109
X13	4.522	4.261	4.410
X14	8.608	3.421	6.386
X15	13.359	6.333	10.349
X16	1.382	8.558	4.456

4.2. Historical Fitting Performance of the SD Model

Historical fitting performance varied across the six variables during 2014–2023 (Figure 7). Population had a MAPE of 0%. GDP had a MAPE of 2.602% and an R^2 of

0.94743. Total water use had a MAPE of 2.728% and an R^2 of 0.33358. Total water supply had a MAPE of 4.058% and an R^2 of −0.66352. Wastewater discharge had a MAPE of 4.062% and an R^2 of 0.77198. COD discharge had a MAPE of 18.966% and an R^2 of 0.59131, the largest overall relative fitting error among the six variables. Some annual absolute relative errors exceeded 10%. Full metrics and yearly errors are reported in Appendix A, Tables A4 and A5. The negative R^2 for total water supply indicates that its squared fitting error exceeded the variation around the observed mean. These results describe in-sample historical fitting and do not show out-of-sample predictive validity.

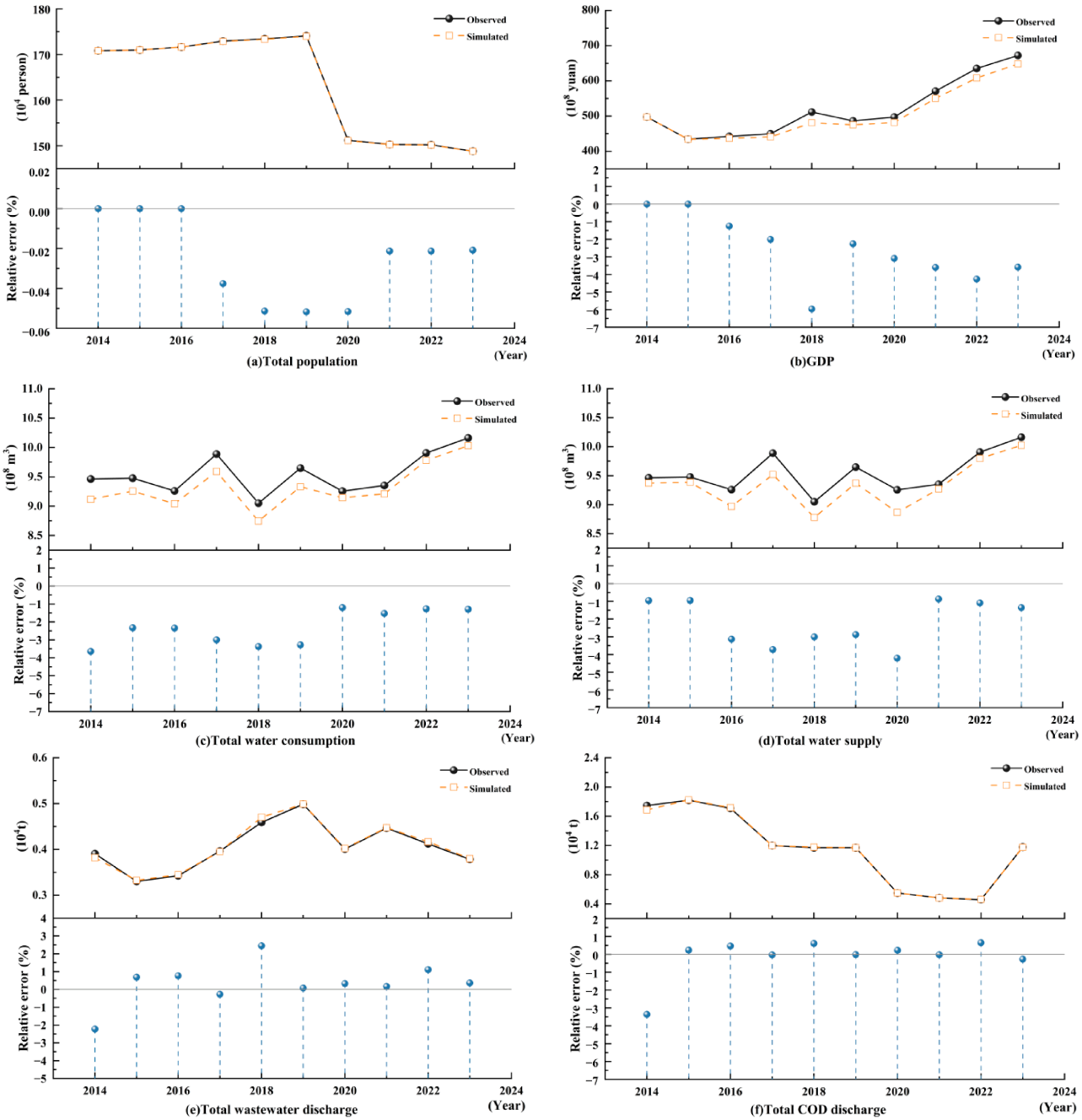


Figure 7. Historical fitting of representative variables in the Baiyin WRCC system, 2014–2023.

The SD equations were also run in a separate numerical implementation. The results were compared with the simulation outputs stored in the original dataset. The maximum relative differences were 0.0514% for 2014–2023 and 0.0011% for the 2024–2035 baseline

simulation. The stored historical population values match the observed data, while a new run of the population equation gives small differences. Population growth inputs and feedback terms both affect this equation.

The model was also tested under seven changes in selected parameters. A 10% reduction in irrigation water use per unit area reduced total water use in 2035 by 7.66%. A 12% reduction in industrial water-use intensity reduced wastewater discharge by 4.35%. A 10% reduction in the domestic COD coefficient reduced total COD discharge by 9.57%. The full results are presented in Appendix A, Table A8.

4.3. Historical Changes in WRCC from 2014 to 2023

According to the cloud model classification, Baiyin's WRCC improved overall during 2014–2023, and the carrying capacity grade rose from Grade IV to Grade II (Tables 5 and 6; Figures 8 and 9). The WRCC values in 2014 and 2015 were 0.371 and 0.387, respectively, corresponding to Grade IV, or the Marginally overloaded status. From 2016 to 2018, the WRCC values increased from 0.481 to 0.578, moving into Grade III, or the Acceptable status. The increase was not continuous over the whole period. From 2019 to 2021, the WRCC values fluctuated between 0.503 and 0.539, and remained within Grade III. This interrupted the upward trend before 2019. In 2022 and 2023, the WRCC values increased to 0.624 and 0.635, respectively, reaching Grade II, or the Good status. Overall, the WRCC value increased from 0.371 in 2014 to 0.635 in 2023. The fluctuation during 2019–2021 shows that the improvement in WRCC was not linear.

Table 6. WRCC evaluation results for Baiyin City, 2014–2023.

Year	WRCC Value	Grade
2014	0.371	IV
2015	0.387	IV
2016	0.481	III
2017	0.510	III
2018	0.578	III
2019	0.532	III
2020	0.539	III
2021	0.503	III
2022	0.624	II
2023	0.635	II

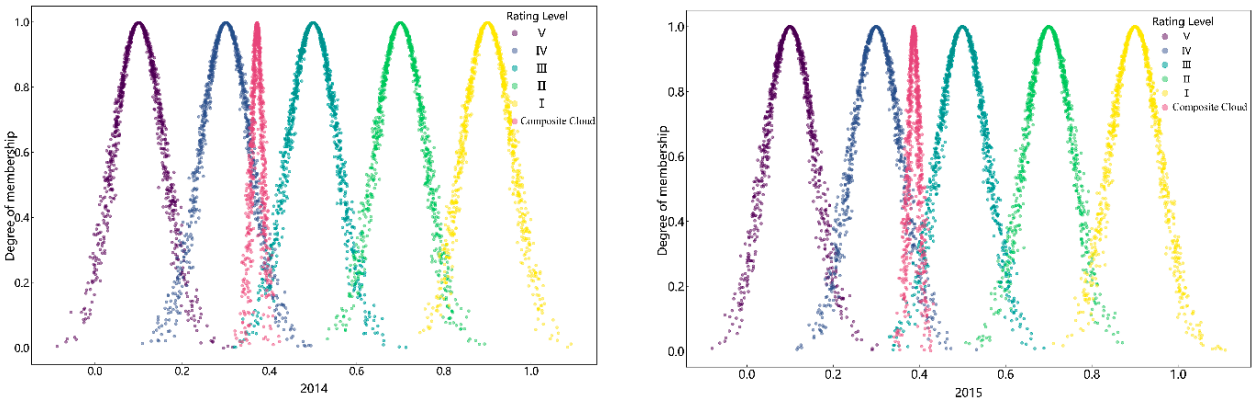


Figure 8. *Cont.*

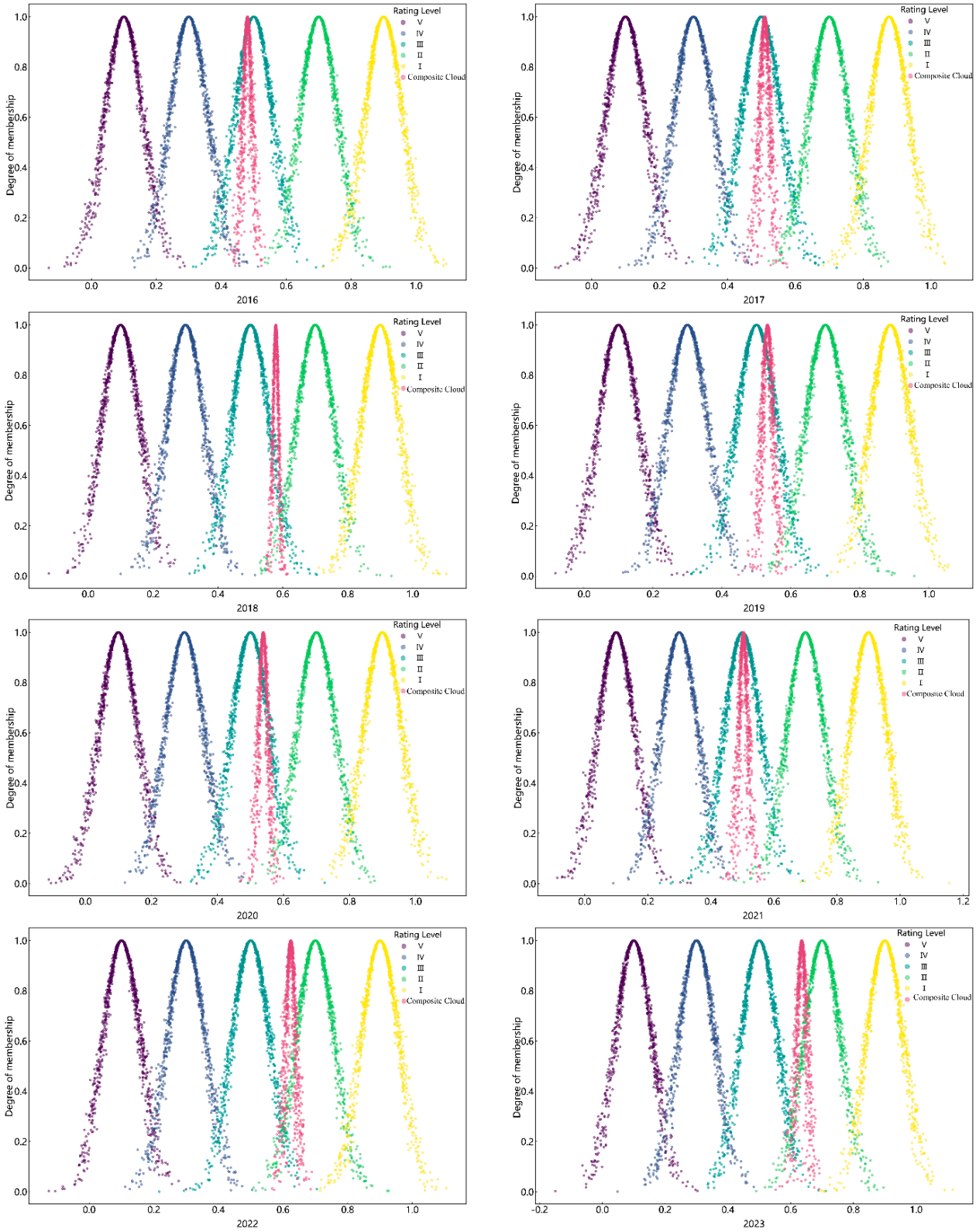


Figure 8. Cloud model evaluation of WRCC in Baiyin City, 2014–2023.

The cloud-model classifications were identical to the corresponding fixed-threshold classifications for all ten historical years (Appendix A, Table A3).

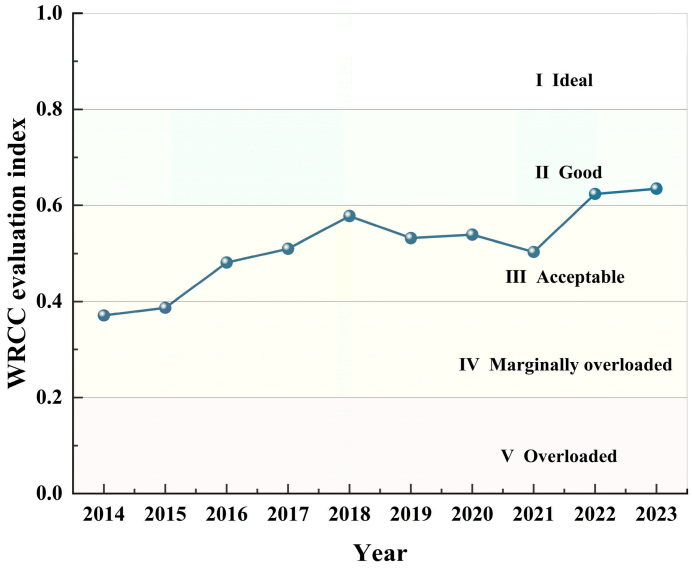


Figure 9. Evolution of WRCC values and carrying capacity grades in Baiyin City, 2014–2023.

4.4. Scenario Simulation of Future WRCC

During the scenario simulation period, total population showed a declining trend, with only small differences among the four scenarios (Figure 10a). GDP increased under all scenarios, with the fastest growth under the economic development scenario, followed by the sustainable development scenario (Figure 10b). The natural development and water-saving scenarios showed lower GDP growth. Total water use increased overall, while total water supply declined after reaching a temporary peak (Figure 10c,d). Water demand grew fastest under the economic development scenario. Growth was slower under the water-saving and sustainable development scenarios. Wastewater discharge and COD discharge showed clearer differences among scenarios (Figure 10e,f). The economic development scenario showed higher wastewater and COD discharge in the stored simulation results. The water-saving and sustainable development scenarios showed lower pollution discharge. In the SD model, COD discharge depends on industrial and domestic wastewater flows and their COD discharge coefficients. The wastewater treatment rate affects reclaimed water supply but does not directly enter the COD discharge equation. The simulated WRCC values from 2024 to 2035 remained close to Grade II under most scenarios, although clear differences appeared under the specified settings (Table 7; Figure 11). By 2035, the water-saving scenario had the highest WRCC value (0.705), followed by the sustainable development scenario (0.655), the natural development scenario (0.643), and the economic development scenario (0.596). The WRCC value under the water-saving scenario was 0.109 higher than that under the economic development scenario, 0.062 higher than that under the natural development scenario, and 0.050 higher than that under the sustainable development scenario. Under the parameter settings of this study, reducing water-use intensity and pollution load led to higher WRCC than increasing economic growth parameters alone.

Table 7. Simulated WRCC values under different development scenarios, 2024–2035.

Year	Natural Development Scenario	Economic Development Scenario	Water-Saving Scenario	Sustainable Development Scenario
2024	0.626	0.575	0.674	0.647
2025	0.623	0.572	0.676	0.649
2026	0.628	0.577	0.679	0.642
2027	0.629	0.583	0.685	0.645

Table 7. *Cont.*

Year	Natural Development Scenario	Economic Development Scenario	Water-Saving Scenario	Sustainable Development Scenario
2028	0.628	0.585	0.685	0.643
2029	0.634	0.590	0.697	0.647
2030	0.637	0.594	0.697	0.650
2031	0.635	0.595	0.700	0.653
2032	0.639	0.593	0.703	0.653
2033	0.642	0.593	0.701	0.649
2034	0.636	0.595	0.706	0.651
2035	0.643	0.596	0.705	0.655

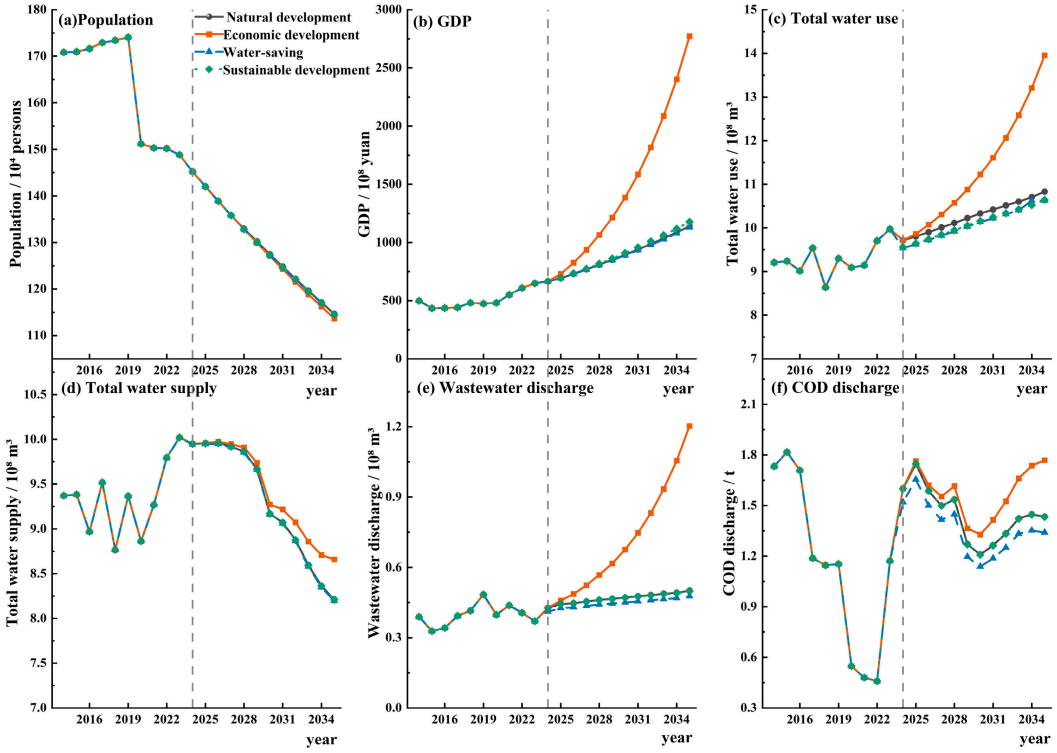


Figure 10. Simulated changes in key variables of the Baiyin WRCC system under different development scenarios, 2014–2035.

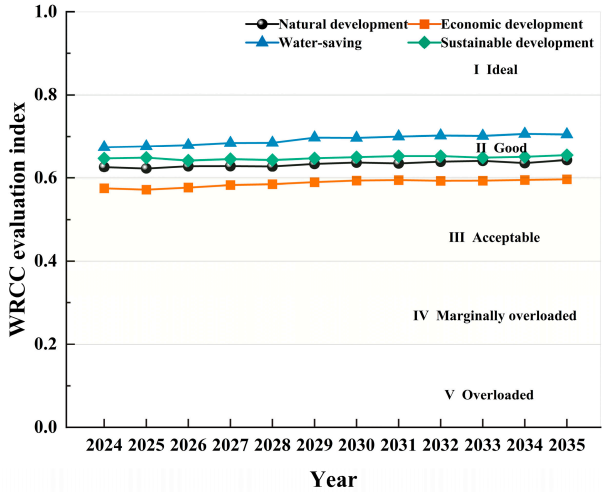


Figure 11. Evolution of simulated WRCC values under different development scenarios, 2024–2035.

5. Discussion

5.1. Historical Changes in WRCC and Possible System Responses

The WRCC of Baiyin City increased from 0.371 in 2014 to 0.635 in 2023, and the carrying capacity grade improved from Grade IV to Grade II. This change suggests that water use and environmental management improved during the study period. It does not mean, however, that the natural water constraint has disappeared. Baiyin still has low precipitation, strong evaporation, and limited per capita water resources. The improvement in WRCC is more likely related to better water-use efficiency, stronger pollution control, greater use of reclaimed water, and gradual adjustment of the local socio-economic system to water scarcity. Similar relationships between water-use efficiency, industrial structure, pollution control, and water availability have been discussed in previous studies [43,45,47].

The change in WRCC was not steady. From 2019 to 2021, the WRCC remained in Grade III and showed clear fluctuations. One possible reason is that changes in economic activity, water demand, and pollution pressure occurred faster than changes in water-saving and treatment capacity. Such time lags are also consistent with the feedback structure of water-resource systems described in SD studies [38,52]. The present study cannot identify a specific causal event behind this fluctuation. The return to Grade II in 2022 and 2023 therefore indicates an improvement within the selected indicator system, rather than a complete removal of water-resource risk [15,53,54].

5.2. Resource Endowment, Development Pressure, and Water Environmental Feedback

Per capita water resources (X1), the water resources development and utilization rate (X5), and COD discharge (X15) together accounted for 37.049% of the total weight. These indicators represent three main aspects of the WRCC system: resource endowment, development pressure, and water environmental pressure. Per capita water resources had the highest weight, showing the importance of natural water availability in the composite index. Similar results have been reported for arid areas in northwest China, where development is strongly limited by water-resource endowment [55].

For Baiyin, increasing water supply may reduce short-term pressure, but it cannot fully solve the basic problem of water scarcity. Improving water-use efficiency is therefore important for long-term WRCC. The relatively high weights of X5 and X15 also show that carrying capacity depends on how intensively water is used and how much pollution is produced after use. A high water resources development and utilization rate leaves less room for the water system to respond to additional demand. High COD discharge can reduce water quality and increase the cost of pollution control.

Economic development can affect WRCC in different ways. Investment in technology, infrastructure, and management can improve water-use efficiency and pollution control. At the same time, growth based on high water consumption and high pollution discharge can increase pressure on the water system [44,45]. Water ecological conditions also influence ecosystem services and the capacity of water bodies to support human activities [48]. For this reason, water supply, pollution control, wastewater treatment, reclaimed water use, and industrial water efficiency should be considered together rather than managed as separate issues.

5.3. Scenario Differences and Development Pathway Choices

The scenario results show a clear ranking in 2035: the water-saving scenario had the highest WRCC value at 0.705, followed by the sustainable development scenario at 0.655, the natural development scenario at 0.643, and the economic development scenario at 0.596. This ranking reflects the parameter settings used in the model and should be understood as a comparison among the four scenarios rather than as a general prediction.

The water-saving scenario performed best mainly because it reduced water-use intensity and pollution pressure at the same time. Agricultural, industrial, and domestic water-use quotas were lower, while wastewater and COD discharge coefficients were also reduced. These changes lowered both total water demand and pollution pressure. This result is consistent with previous SD studies showing that water-saving measures, population management, and better supply structures can reduce pressure on regional water resources [10,11].

The economic development scenario had the lowest WRCC under the specified settings. In this scenario, faster industrial growth, urbanization, and domestic demand increased both water use and pollution pressure. These effects partly offset the positive contribution of economic development. This suggests that economic growth alone does not necessarily improve WRCC when water-use efficiency and pollution control do not improve at the same pace. Similar relationships have also been discussed in previous studies [45,47,56].

The sustainable development scenario performed better than the natural development scenario but worse than the water-saving scenario. This does not mean that sustainable development is less desirable. Under the settings used here, the sustainable development scenario combines stronger water-saving measures with continued economic growth. In this scenario, economic growth also increases water use and wastewater generation. These changes can offset part of the improvement associated with lower water-use intensity. The comparison therefore shows the importance of balancing development goals with water demand and pollution control [49,50].

5.4. Implications for Arid and Semi-Arid Resource-Based Industrial Cities

The Baiyin case shows that WRCC in resource-based industrial cities depends on more than water supply alone. Natural water availability, industrial and agricultural demand, water-use efficiency, and pollution pressure all need to be considered together. Under the scenario settings used in this study, demand-side water saving, industrial water-use efficiency, reclaimed water use, and pollution reduction all contribute to higher WRCC. Agricultural water-saving irrigation, industrial water-saving technology, wastewater treatment, and water reuse may therefore be combined in water-management practice. Their actual effects will still depend on local conditions.

The results also point to a change in water-management priorities. For cities with limited water resources, development cannot rely only on increasing supply. Water demand, industrial growth, agricultural production, and ecological restoration also need to remain within local water and environmental limits. The good performance of the water-saving scenario does not mean that economic development should simply be restricted. It shows that reducing water-use intensity and pollution load can help create more space for development under water scarcity. If future growth continues to depend heavily on water-intensive and pollution-intensive activities, further improvement in WRCC will be more difficult.

6. Conclusions

This study used an integrated approach combining system dynamics modelling and the cloud model to assess water resources carrying capacity (WRCC) in Baiyin City. Baiyin represents a typical arid and semi-arid resource-based industrial city where water scarcity, industrial demand, and water environmental pressure occur at the same time. In the composite index, per capita water resources (X1), the water resources development and utilization rate (X5), and COD discharge (X15) had the highest weights, together accounting for 37.049% of the total weight. From 2014 to 2023, WRCC increased from 0.371 to 0.635, and the carrying capacity grade improved from Grade IV to Grade II. The overall trend was upward, although clear fluctuations occurred during 2019–2021. These changes suggest an

improvement in the balance among water use, economic development, and environmental management during the study period. The causes of the short-term fluctuations cannot be identified from the present analysis.

The scenario results show clear differences among the four development pathways. In 2035, the simulated WRCC values were 0.705 under the water-saving scenario, 0.655 under the sustainable development scenario, 0.643 under the natural development scenario, and 0.596 under the economic development scenario. The water-saving scenario was 0.109 higher than the economic development scenario. Under the model settings used in this study, reducing water-use intensity and pollution pressure produced better WRCC outcomes than increasing economic growth parameters alone. For Baiyin and similar water-constrained industrial cities, water management should give more attention to demand-side water saving, industrial water-use efficiency, reclaimed water use, and pollution control.

The results should be understood as conditional on the selected indicator system, model structure, and scenario settings. The local sensitivity analysis examined how key model outputs respond to selected parameter changes. Independent temporal validation and a full uncertainty analysis were not included in this assessment. Strong correlations among some indicators may also create redundancy. The results may also depend on the normalization rules and the selected grade boundaries. Future studies could further examine climate change, extreme drought, policy adjustment, and industrial restructuring.

Author Contributions: Conceptualization, H.S.; methodology, R.Z. and N.L.; formal analysis, S.Y.; resources, Y.S.; data curation, N.L. and Y.S.; writing—original draft preparation, S.Y.; writing—review and editing, R.Z. and S.Y.; supervision, H.S.; project administration, R.Z.; funding acquisition, R.Z. All authors have read and agreed to the published version of the manuscript.

Funding: This research was funded by the Gansu Provincial Water Conservancy Scientific Research, Experimentation and Technology Extension Program (Grant Nos. 24GSLK017, 26GSLK015, and 26GSLK034).

Institutional Review Board Statement: Not applicable.

Informed Consent Statement: Not applicable.

Data Availability Statement: The data supporting the findings of this study are available from the corresponding author upon reasonable request. Additional supporting information is provided in Appendix A.

Conflicts of Interest: The authors declare no conflicts of interest.

Appendix A. Supporting Methodological and Reproducibility Information

Appendix A.1

Table A1. Comparative summary of representative WRCC studies and the present study.

Study	Study Area	Main Method(s)	Dynamic/Scenario Component	Main Analytical Focus
Xu et al. (2024) [7]	Beijing–Tianjin–Hebei urban agglomeration	Improved principal component analysis	WRCC prediction	Regional WRCC changes
Liu and Liu (2023) [8]	Liaoning Province	TOPSIS and GIS	Not reported	Spatial-temporal WRCC differentiation
Jia et al. (2023) [9]	Cele–Yutian Oasis	DPSR, TOPSIS, obstacle degree, and Markov	Markov component	WRCC and land use change

Table A1. *Cont.*

Study	Study Area	Main Method(s)	Dynamic/Scenario Component	Main Analytical Focus
Sun and Yang (2019) [10]	Xiong'an New Area	SD model	Dynamic WRCC simulation	WRCC changes
Yang et al. (2019) [11]	Xi'an City	AHP and SD	SD scenario simulation	WRCC evaluation and scenario comparison
This study	Baiyin City	Combined AHP–entropy weighting and cloud-based grade classification	SD scenario simulation	Historical assessment linked with exploratory scenario comparison

The comparison uses only information stated in the current manuscript. Not reported indicates a component not described in that summary.

Appendix A.2

Table A2. Pearson correlation matrix of the 16 WRCC indicators, 2014–2023.

Indicator	X1	X2	X3	X4	X5	X6	X7	X8
X1	1.000	0.989	−0.796	−0.636	−0.923	0.739	−0.658	−0.713
X2	0.989	1.000	−0.866	−0.709	−0.955	0.770	−0.736	−0.784
X3	−0.796	−0.866	1.000	0.780	0.946	−0.833	0.880	0.889
X4	−0.636	−0.709	0.780	1.000	0.693	−0.409	0.769	0.709
X5	−0.923	−0.955	0.946	0.693	1.000	−0.901	0.849	0.896
X6	0.739	0.770	−0.833	−0.409	−0.901	1.000	−0.765	−0.876
X7	−0.658	−0.736	0.880	0.769	0.849	−0.765	1.000	0.961
X8	−0.713	−0.784	0.889	0.709	0.896	−0.876	0.961	1.000
X9	−0.657	−0.728	0.851	0.606	0.861	−0.906	0.886	0.973
X10	0.426	0.512	−0.719	−0.437	−0.697	0.802	−0.811	−0.876
X11	0.559	0.596	−0.583	−0.518	−0.652	0.568	−0.675	−0.703
X12	0.227	0.196	−0.041	−0.000	−0.091	−0.038	0.109	0.123
X13	−0.794	−0.844	0.898	0.631	0.947	−0.945	0.909	0.977
X14	−0.006	−0.028	0.123	0.098	0.133	−0.107	0.339	0.235
X15	0.473	0.538	−0.711	−0.583	−0.686	0.652	−0.882	−0.804
X16	−0.026	−0.119	0.278	0.695	0.117	0.141	0.514	0.343
X1	−0.657	0.426	0.559	0.227	−0.794	−0.006	0.473	−0.026
X2	−0.728	0.512	0.596	0.196	−0.844	−0.028	0.538	−0.119
X3	0.851	−0.719	−0.583	−0.041	0.898	0.123	−0.711	0.278
X4	0.606	−0.437	−0.518	−0.000	0.631	0.098	−0.583	0.695
X5	0.861	−0.697	−0.652	−0.091	0.947	0.133	−0.686	0.117
X6	−0.906	0.802	0.568	−0.038	−0.945	−0.107	0.652	0.141
X7	0.886	−0.811	−0.675	0.109	0.909	0.339	−0.882	0.514
X8	0.973	−0.876	−0.703	0.123	0.977	0.235	−0.804	0.343
X9	1.000	−0.934	−0.727	0.099	0.971	0.232	−0.734	0.218
X10	−0.934	1.000	0.785	−0.042	−0.863	−0.472	0.769	−0.238
X11	−0.727	0.785	1.000	0.332	−0.723	−0.715	0.719	−0.326
X12	0.099	−0.042	0.332	1.000	0.022	−0.413	0.158	0.103
X13	0.971	−0.863	−0.723	0.022	1.000	0.230	−0.769	0.164
X14	0.232	−0.472	−0.715	−0.413	0.230	1.000	−0.645	0.333
X15	−0.734	0.769	0.719	0.158	−0.769	−0.645	1.000	−0.449
X16	0.218	−0.238	−0.326	0.103	0.164	0.333	−0.449	1.000

N = 10 annual observations. The matrix is shown in two column groups, X1–X8 and X9–X16. Values are displayed to three decimals. Strong correlations do not establish conceptual duplication or causal effects.

Appendix A.3

Table A3. Comparison between cloud-model and fixed-threshold classifications, 2014–2023.

Year	WRCC Value	Cloud-Model Grade	Fixed-Threshold Grade	Agreement
2014	0.371	IV	IV	Yes
2015	0.387	IV	IV	Yes
2016	0.481	III	III	Yes
2017	0.510	III	III	Yes
2018	0.578	III	III	Yes
2019	0.532	III	III	Yes
2020	0.539	III	III	Yes
2021	0.503	III	III	Yes
2022	0.624	II	II	Yes
2023	0.635	II	II	Yes

The comparison uses the reported historical classifications. Agreements = 10/10. Agreement rate = 100%. Fixed intervals are those in Table 3.

Appendix A.4

Table A4. Historical fitting performance of the SD model, 2014–2023.

Variable	Unit	MAE	RMSE	MAPE (%)	R^2	Maximum Absolute Relative Error (%)
Population	10^4 persons	0.000000	0.000000	0.000	1.00000	0.000
GDP	10^8 yuan	14.319390	17.715972	2.602	0.94743	5.960
Total water use	10^8 m^3	0.259514	0.270480	2.728	0.33358	4.519
Total water supply	10^8 m^3	0.406307	0.588364	4.058	−0.66352	13.633
Wastewater discharge	10^8 m^3	0.015565	0.026033	4.062	0.77198	20.564
COD discharge	10^4 tonnes	0.317988	0.424703	18.966	0.59131	53.145

Each series contains 10 annual observations. MAE and RMSE use the listed units. These are in-sample historical fitting metrics. COD values are in 10^4 t.

Appendix A.5

Table A5. Historical observations, simulated values, and yearly relative errors of representative SD variables, 2014–2023.

Variable	Year	Observed	Simulated	Relative Error (%)
Population	2014	170.830000000	170.830000000	0.000000
	2015	170.990000000	170.990000000	0.000000
	2016	171.640000000	171.640000000	0.000000
	2017	172.930000000	172.930000000	0.000000
	2018	173.420000000	173.420000000	0.000000
	2019	174.080000000	174.080000000	0.000000
	2020	151.210000000	151.210000000	0.000000
	2021	150.300000000	150.300000000	0.000000
	2022	150.210000000	150.210000000	0.000000
	2023	148.810000000	148.810000000	0.000000

Table A5. *Cont.*

Variable	Year	Observed	Simulated	Relative Error (%)
GDP	2014	497.579600000	497.580000000	0.000080
	2015	434.280000000	434.280000000	0.000000
	2016	442.213000000	436.676000000	−1.252112
	2017	449.899900000	440.872000000	−2.006646
	2018	511.596600000	481.104000000	−5.960282
	2019	486.340000000	475.350000000	−2.259736
	2020	497.260000000	481.911000000	−3.086715
	2021	571.020000000	550.476000000	−3.597772
	2022	635.600000000	608.435000000	−4.273914
	2023	672.300000000	648.212000000	−3.582924
Total water use	2014	9.462800000	9.206890000	−2.704379
	2015	9.475900000	9.239440000	−2.495383
	2016	9.258900000	9.014620000	−2.638326
	2017	9.886800000	9.543050000	−3.476858
	2018	9.050100000	8.641150000	−4.518735
	2019	9.647698374	9.301370000	−3.589751
	2020	9.255113878	9.089190000	−1.792781
	2021	9.352600000	9.144660000	−2.223339
	2022	9.906758647	9.708700000	−1.999228
	2023	10.161600000	9.974060000	−1.845575
Total water supply	2014	9.462800000	9.372630000	−0.952889
	2015	9.475900000	9.385620000	−0.952733
	2016	9.258900000	8.968570000	−3.135686
	2017	9.886800000	9.518940000	−3.720719
	2018	9.050100000	8.764950000	−3.150794
	2019	9.647500000	9.366660000	−2.911013
	2020	9.808000000	8.863270000	−9.632239
	2021	10.733580000	9.270250000	−13.633196
	2022	9.905200000	9.795120000	−1.111335
	2023	10.161600000	10.021300000	−1.380688
Wastewater discharge	2014	0.390590000	0.388657000	−0.494892
	2015	0.330200000	0.328350000	−0.560267
	2016	0.342400000	0.340990000	−0.411799
	2017	0.326100000	0.393158000	20.563631
	2018	0.459007920	0.415552000	−9.467357
	2019	0.498600000	0.484584000	−2.811071
	2020	0.400800000	0.397636000	−0.789421
	2021	0.446700000	0.437827000	−1.986344
	2022	0.412200000	0.405955000	−1.515041
	2023	0.378300000	0.370650000	−2.022205
COD discharge	2014	2.357000000	1.733610000	−26.448451
	2015	2.267600000	1.816890000	−19.876080
	2016	2.320000000	1.708830000	−26.343534
	2017	1.850000000	1.188650000	−35.748649
	2018	1.230000000	1.145550000	−6.865854
	2019	1.170000000	1.153380000	−1.420513
	2020	1.170000000	0.548205000	−53.144872
	2021	0.560000000	0.479978000	−14.289643
	2022	0.482944000	0.458834000	−4.992297
	2023	1.178588000	1.172320000	−0.531823

Units are those listed in Table A4. Relative error = (simulated − observed)/observed × 100%. Total water use and total water supply observations were restored from archived indicators and observed GDP or population, respectively. Archived simulations were not changed.

Appendix A.6

Table A6. Key equations, parameters, units, and initial conditions of the SD model.

Variable/Parameter	Type	Equation/Value	Unit	Initial Value	Source/Basis
total_population	Stock	INTEG (population_increase, 170.83)	10^4 persons	170.83	Archived mdl
population_growth_rate	Lookup	Lookup (Time)	Dmnl	n.a.	Archived mdl
GDP	Auxiliary	primary_industry_value_added + tertiary_industry_value_added + secondary_industry_value_added	10^8 yuan	n.a.	Archived mdl
primary_industry_value_added	Stock	INTEG (primary_industry_value_added_increase, 57.1098)	10^8 yuan	57.1098	Archived mdl
secondary_industry_value_added	Stock	INTEG (secondary_industry_value_added_increase, 251.05)	10^8 yuan	251.05	Archived mdl
tertiary_industry_value_added	Stock	INTEG (tertiary_industry_value_added_increase, 189.42)	10^8 yuan	189.42	Archived mdl
total_water_resources	Auxiliary	groundwater_resources + surface_water_resources-double_counted_water_volume	10^8 m^3	n.a.	Archived mdl
total_water_supply	Auxiliary	reclaimed_water_reuse + groundwater_supply + surface_water_supply	10^8 m^3	n.a.	Archived mdl
total_water_use	Auxiliary	agricultural_water_use + industrial_water_use + ecological_water_use + domestic_water_use	10^8 m^3	n.a.	Archived mdl
agricultural_water_use	Auxiliary	agricultural_irrigation_water_use + orchard_irrigation_water_use + livestock_water_use + grassland_irrigation_water_use	10^8 m^3	n.a.	Archived mdl
industrial_water_use	Auxiliary	water_use_per_CNY_10,000_industrial_value_added*industrial_value_added*0.0001	10^8 m^3	n.a.	Archived mdl
domestic_water_use	Auxiliary	rural_domestic_water_use + urban_domestic_water_use	10^8 m^3	n.a.	Archived mdl
ecological_water_use	Lookup	Lookup (Time)	10^8 m^3	n.a.	Archived mdl
total_wastewater_discharge	Auxiliary	industrial_wastewater_discharge + domestic_wastewater_discharge	10^8 m^3	n.a.	Archived mdl
wastewater_treatment_rate	Lookup	Lookup (Time)	Dmnl	n.a.	Archived mdl
treated_wastewater_volume	Auxiliary	total_wastewater_discharge*wastewater_treatment_rate	10^8 m^3	n.a.	Archived mdl

Table A6. *Cont.*

Variable/Parameter	Type	Equation/Value	Unit	Initial Value	Source/Basis
reclaimed_water_reuse	Auxiliary	treated_wastewater_volume*reclaimed_water_treatment_rate	10^8 m^3	n.a.	Archived mdl
reclaimed_water_treatment_rate	Lookup	Lookup (Time)	Dmnl	n.a.	Archived mdl
total_COD_discharge	Auxiliary	industrial_wastewater_COD_discharge + domestic_wastewater_COD_discharge	10^4 t	n.a.	Archived mdl
water_use_per_CNY_10,000_industrial_value_added	Lookup	Lookup (Time)	m^3 per 10,000 CNY	n.a.	Archived mdl
domestic_wastewater_discharge_coefficient	Lookup	Lookup (Time)	Dmnl	n.a.	Archived mdl
industrial_wastewater_discharge_coefficient	Lookup	Lookup (Time)	Dmnl	n.a.	Archived mdl
domestic_wastewater_COD_coefficient	Lookup	Lookup (Time)	Dmnl	n.a.	Archived mdl
industrial_wastewater_COD_coefficient	Lookup	Lookup (Time)	Dmnl	n.a.	Archived mdl

Equations and initial conditions are based on the archived model. Time-varying lookup series are retained in the archived .mdl file. The original calibration procedure is not fully preserved. These materials support model implementation checks rather than independent validation.

Appendix A.7

Table A7. Historical WRCC scores under different weighting schemes, 2014–2023.

Year	AHP Score	AHP Grade	Entropy Score	Entropy Grade	Combined Score	Combined Grade
2014	0.3684	IV	0.3757	IV	0.3715	IV
2015	0.3804	IV	0.3959	IV	0.3870	IV
2016	0.4687	III	0.4970	III	0.4809	III
2017	0.5006	III	0.5228	III	0.5101	III
2018	0.6247	II	0.5165	III	0.5783	III
2019	0.5126	III	0.5576	III	0.5319	III
2020	0.5078	III	0.5804	III	0.5389	III
2021	0.4712	III	0.5459	III	0.5032	III
2022	0.5988	III	0.6575	II	0.6239	II
2023	0.5953	III	0.6890	II	0.6354	II

Note: Scores were calculated using the stored historical evaluation inputs and the three published weighting vectors. Grades follow Table 3. This is an input-level comparison, not a reconstruction of the original standardization and cloud-model procedures.

Appendix A.8

Table A8. Local sensitivity of selected SD model outputs in 2035.

Parameter Change	Model Output	Change in 2035 (%)
Irrigation water use per unit area −10%	Total water use	−7.664
Industrial water-use intensity −12%	Wastewater discharge	−4.348
Industrial water-use intensity +8%	Wastewater discharge	+2.899
Wastewater treatment rate set to 0.95	Total water supply	−0.067
Wastewater treatment rate set to 1.00	Total water supply	+0.134
Domestic COD coefficient −10%	Total COD discharge	−9.575
Domestic COD coefficient +5%	Total COD discharge	+4.787

Note: The tests were applied to the baseline SD model from 2024 onward. All historical inputs were kept unchanged. The results describe local parameter responses and do not test the stability of WRCC rankings across the four development scenarios.

References

1. Gleick, P.H. Global freshwater resources: Soft-path solutions for the 21st century. *Science* **2003**, *302*, 1524–1528. [CrossRef] [PubMed]
2. Mekonnen, M.M.; Hoekstra, A.Y. Four billion people facing severe water scarcity. *Sci. Adv.* **2016**, *2*, e1500323. [CrossRef] [PubMed]
3. Vörösmarty, C.J.; McIntyre, P.B.; Gessner, M.O.; Dudgeon, D.; Prusevich, A.; Green, P.; Glidden, S.; Bunn, S.E.; Sullivan, C.A.; Liermann, C.R.; et al. Global threats to human water security and river biodiversity. *Nature* **2010**, *467*, 555–561, Erratum in *Nature* **2010**, *468*, 334. https://doi.org/10.1038/nature09440. [CrossRef] [PubMed]
4. Li, Q.S.; Liu, Z.H.; Yang, Y.H.; Han, Y.; Wang, X.P. Evaluation of water resources carrying capacity in Tarim River Basin under game theory combination weights. *Ecol. Indic.* **2023**, *154*, 110609. [CrossRef]
5. Meng, L.; Chen, Y.; Li, W.; Zhao, R. Fuzzy comprehensive evaluation model for water resources carrying capacity in Tarim River Basin, Xinjiang, China. *Chin. Geogr. Sci.* **2009**, *19*, 89–95. [CrossRef]
6. Zuo, Q.T.; Guo, J.; Ma, J.; Cui, G.; Yang, R.; Yu, L. Assessment of regional-scale water resources carrying capacity based on fuzzy multiple attribute decision-making and scenario simulation. *Ecol. Indic.* **2021**, *130*, 108034. [CrossRef]
7. Xu, W.T.; Jin, J.; Zhang, J.; Yuan, S.; Tang, M.; Liu, Y.; Guan, T. Prediction of regional water resources carrying capacity based on stochastic simulation: A case study of the Beijing–Tianjin–Hebei urban agglomeration. *J. Hydrol. Reg. Stud.* **2024**, *56*, 101976. [CrossRef]
8. Liu, M.; Liu, L. Study on spatial-temporal differentiation of water resources carrying capacity evaluation in Liaoning Province. *Water Resour.* **2023**, *50*, 857–867. [CrossRef]
9. Jia, G.W.; Li, S.; Jie, F.; Ge, Y.; Liu, N.; Liang, F. Assessing water resource carrying capacity and sustainability in the Cele–Yutian Oasis, China: A TOPSIS–Markov model analysis. *Water* **2023**, *15*, 3652. [CrossRef]
10. Sun, B.; Yang, X. Simulation of water resources carrying capacity in Xiong'an New Area based on a system dynamics model. *Water* **2019**, *11*, 1085. [CrossRef]
11. Yang, Z.; Song, J.; Cheng, D.; Xia, J.; Li, Q.; Ahamad, M.I. Comprehensive evaluation and scenario simulation for the water resources carrying capacity in Xi'an City, China. *J. Environ. Manag.* **2019**, *230*, 221–233. [CrossRef] [PubMed]
12. Barati, A.A.; Pour, M.D.; Sardooei, M.A. Water crisis in Iran: A system dynamics approach on water, energy, food, land and climate (WEFLC) nexus. *Sci. Total Environ.* **2023**, *882*, 163549. [CrossRef] [PubMed]
13. Dai, D.; Sun, M.D.; Xu, X.Q.; Lei, K. Assessment of the water resource carrying capacity based on the ecological footprint: A case study in Zhangjiakou City, North China. *Environ. Sci. Pollut. Res.* **2019**, *26*, 11000–11011. [CrossRef] [PubMed]
14. Li, D.; Liu, C.; Gan, W. A new cognitive model: Cloud model. *Int. J. Intell. Syst.* **2009**, *24*, 357–375. [CrossRef]
15. Cao, W.; Deng, J.; Yang, Y.; Zeng, Y.; Liu, L. Water carrying capacity evaluation method based on cloud model theory and an evidential reasoning approach. *Mathematics* **2022**, *10*, 266. [CrossRef]
16. Zhou, K. Comprehensive evaluation on water resources carrying capacity based on improved AGA-AHP method. *Appl. Water Sci.* **2022**, *12*, 103. [CrossRef]
17. Li, J.Y. Evaluation methods for water resource suitability in territorial spatial planning: A case study of Baiyin City in a semi-arid region. *Int. J. Environ. Res. Public Health* **2022**, *19*, 12973. [CrossRef] [PubMed]
18. Wang, H.F. Sustainable development strategy of Baiyin City from the perspective of the Lanzhou–Baiyin metropolitan economic circle. *Econ. Geogr.* **2011**, *31*, 566–572.

19. Zhang, H.R.; Xu, K.N.; Guo, F.; Liu, A. Sustainable utilization of water resources in the Yellow River Basin based on water resources ecological footprint. *J. Environ. Eng. Technol.* **2024**, *14*, 1732–1742. [CrossRef]
20. Wang, H.; Qin, D.Y.; Wang, J.H.; Li, L.Y. Water resources carrying capacity in inland arid areas of Northwest China. *J. Nat. Resour.* **2004**, *19*, 151–159. [CrossRef]
21. Li, J.H.; Xia, F.Q.; Yang, D.G.; Huo, J.W. Comprehensive evaluation of water resource carrying capacity in Northwest China. *Water* **2025**, *17*, 67. [CrossRef]
22. Sun, Y.S.; Wang, Y.L.; Zhang, W.; Ye, S.G. Regional water resources carrying capacity in China based on analytic hierarchy process and system dynamics model: A case study of Golmud City. *Front. Environ. Sci.* **2024**, *12*, 1450747. [CrossRef]
23. Dai, C.; Tang, J.; Li, Z.; Duan, Y.; Qu, Y.; Yang, Y.; Lyu, H.; Zhang, D.; Wang, Y. Index System of Water Resources Development and Utilization Level Based on Water-Saving Society. *Water* **2022**, *14*, 802. [CrossRef]
24. Pant, S.; Kumar, A.; Ram, M.; Klochkov, Y.; Sharma, H.K. Consistency Indices in Analytic Hierarchy Process: A Review. *Mathematics* **2022**, *10*, 1206. [CrossRef]
25. Ponsiglione, A.M.; Amato, F.; Cozzolino, S.; Russo, G.; Romano, M.; Improta, G. A Hybrid Analytic Hierarchy Process and Likert Scale Approach for the Quality Assessment of Medical Education Programs. *Mathematics* **2022**, *10*, 1426. [CrossRef]
26. Han, L.; Wang, Y.; Li, S.D.; Li, W.; Chen, X.J. Evaluation of Water Resource Carrying Capacity and Analysis of Driving Factors in the Dadu River Basin Based on the Entropy Weight Method and CRITIC Comprehensive Evaluation Method. *Water* **2025**, *17*, 2360. [CrossRef]
27. Li, W.Z.; Liu, S.S.; Chang, W.J.; Zhang, X.; Li, C.H.; Qin, T.L. Research progress on the evaluation of water resources carrying capacity. *Pol. J. Environ. Stud.* **2023**, *32*, 1975–1986. [CrossRef] [PubMed]
28. Zhu, Y.; Tian, D.; Yan, F. Effectiveness of Entropy Weight Method in Decision-Making. *Math. Probl. Eng.* **2020**, *2020*, 3564835. [CrossRef]
29. Du, L.L.; Niu, Z.; Zhang, R.; Zhang, J.; Jia, L.; Wang, L. Evaluation of water resource carrying potential and barrier factors in Gansu Province based on game theory combined weighting and improved TOPSIS model. *Ecol. Indic.* **2024**, *166*, 112438. [CrossRef]
30. Wang, J.X.; Feng, C.M.; Zhu, J.N.; Zhang, S.H.; Cheng, R. A Combined AHP-Entropy and Game Theory Weighting Approach for Aqueduct Safety Evaluation: A Case Study of the Kezi River Aqueduct. *Appl. Sci.* **2026**, *16*, 2360. [CrossRef]
31. Zhang, H.; Lu, M.; Ke, X.; Yu, S.; Zhao, J.; Wu, Y.; Cheng, L.; Li, X. Evaluation model of black-start schemes based on optimal combination weights and improved VIKOR method. *Int. J. Electr. Power Energy Syst.* **2021**, *129*, 106762. [CrossRef]
32. Zhao, B.; Shao, Y.B.; Yang, C.; Zhao, C. The application of the game theory combination weighting-normal cloud model to the quality evaluation of surrounding rocks. *Front. Earth Sci.* **2024**, *12*, 1346536. [CrossRef]
33. Chang, X.H.; Luo, Q.K. Coal spontaneous combustion hazard extension evaluation in goaf based on improved game theory. *Min. Saf. Environ. Prot.* **2022**, *49*, 211–218. [CrossRef]
34. Pu, J.; Liu, Z. HECM-Plus: Hyper-Entropy Enhanced Cloud Models for Uncertainty-Aware Design Evaluation in Multi-Expert Decision Systems. *Entropy* **2025**, *27*, 475. [CrossRef] [PubMed]
35. Dong, J.; Liu, D.; Liu, Y.; Huo, H.; Dou, X.; Bao, A. Trading performance evaluation for traditional power generation group based on an integrated matter-element extension cloud model. *Energy Rep.* **2021**, *7*, 3074–3089. [CrossRef]
36. Ma, S.Q.; Xie, Y.L.; Qiu, J.L.; Lai, J.X.; Sun, H. An Improved Optimal Cloud Entropy Extension Cloud Model for the Risk Assessment of Soft Rock Tunnels in Fault Fracture Zones. *Buildings* **2025**, *15*, 2700. [CrossRef]
37. Bakhshianlamouki, E.; Masia, S.; Karimi, P.; van der Zaag, P.; Sušnik, J. A system dynamics model to quantify the impacts of restoration measures on the water-energy-food nexus in the Urmia lake Basin, Iran. *Sci. Total Environ.* **2020**, *708*, 134874. [CrossRef] [PubMed]
38. Phan, T.D.; Bertone, E.; Stewart, R.A. Critical review of system dynamics modelling applications for water resources planning and management. *Clean. Environ. Syst.* **2021**, *2*, 100031. [CrossRef]
39. Zhao, W.L.; Ji, Y.H.; Zuo, Q.T.; Fu, Y.Y. Variation in balance between water supply and water demand in Yinqin irrigation district. *J. Irrig. Drain.* **2023**, *42*, 128–135. [CrossRef]
40. Wang, X.Y.; Zhang, Z.; Liu, F.; Chen, S.; Dong, J.; Mao, Y.; Cao, J. Study on Supply-Demand Balance Analysis and Service Flow of Water Resources in Dongjiang River Basin. *Water* **2022**, *14*, 2060. [CrossRef]
41. Nie, H.Y.; Liu, K.X.; Hu, B.H.; Ni, P.P. Research on supply and demand prediction and balance plan of water resources in Xinjiang based on SD model. *Water Sav. Irrig.* **2025**, *8*, 15–21. [CrossRef]
42. Wang, T.; You, J.J.; Ma, Z.Z.; Xiao, P. A Hierarchical Index System for Analysis of Water Supply-Demand Situation. *Water Resour. Manag.* **2022**, *36*, 4485–4498. [CrossRef]
43. Zhu, Q.Y.; Cao, Y. Research on provincial water resources carrying capacity and coordinated development in China based on combined weighting TOPSIS model. *Sci. Rep.* **2024**, *14*, 12497. [CrossRef] [PubMed]
44. Wang, T.; Jian, S.; Wang, J.; Yan, D. Dynamic interaction of water–economic–social–ecological environment complex system under the framework of water resources carrying capacity. *J. Clean. Prod.* **2022**, *368*, 133132. [CrossRef]

45. Wang, X.Y.; Zhang, S.L.; Gao, C.; Tang, X.P. Coupling coordination and driving mechanisms of water resources carrying capacity under the dynamic interaction of the water-social-economic-ecological environment system. *Sci. Total Environ.* **2024**, *920*, 171011. [CrossRef] [PubMed]
46. Buendía Hernández, A.; André, F.J.; Santos-Arteaga, F.J. On the Evolution and Determinants of Water Efficiency in the Regions of Spain. *Water Resour. Manag.* **2024**, *38*, 3093–3112. [CrossRef]
47. Li, F.; Du, J.E.; Li, H.M.; Du, X.W.; Xu, X.Y. Analysis of coupling coordination and spatio-temporal of water resource carrying capacity and regional economic development-taking Henan Province as an example. *Environ. Dev. Sustain.* **2026**, *28*, 17771–17803. [CrossRef]
48. Grizzetti, B.; Liquete, C.; Pistocchi, A.; Vigiak, O.; Zulian, G.; Bouraoui, F.; De Roo, A.; Cardoso, A.C. Relationship between ecological condition and ecosystem services in European rivers, lakes and coastal waters. *Sci. Total Environ.* **2019**, *671*, 452–465. [CrossRef] [PubMed]
49. Chen, X.; Xu, Q.; Cai, J. Research on the urban water resources carrying capacity by using system dynamics simulation. *Hydrol. Res.* **2023**, *54*, 418–434. [CrossRef]
50. Wang, Y.Z.; Wang, J.R.; Duan, X.J.; Wang, L.Q. Assessment and Simulation of Water Environment Carrying Capacity in a River Basin Using System Dynamics Model. *Pol. J. Environ. Stud.* **2023**, *32*, 2893–2907. [CrossRef]
51. Liu, Y.; Gao, C.; Ji, X.; Zhang, Z.; Zhang, Y.; Liu, C.; Wang, Z. Simulation of water resources carrying capacity of the Hangbu River Basin based on system dynamics model and TOPSIS method. *Front. Environ. Sci.* **2022**, *10*, 1045907. [CrossRef]
52. Wang, H.; Huang, J.J.; Cheng, X.J.; Zhou, H.; Yuan, Y.B. Scenario simulation of water resources development and utilization based on a system dynamics model. *Int. J. Water Resour. Dev.* **2022**, *38*, 447–463. [CrossRef]
53. Ren, B.; Zhang, Q.; Ren, J.; Ye, S.; Yan, F. A Novel Hybrid Approach for Water Resources Carrying Capacity Assessment by Integrating Fuzzy Comprehensive Evaluation and Analytical Hierarchy Process Methods with the Cloud Model. *Water* **2020**, *12*, 3241. [CrossRef]
54. Wang, Y.; Nie, S.; Han, W.; Huang, B. Integrated assessment and spatial coordination analysis of water resources carrying capacity in the Changbai mountain headwater region using cloud model and geodetector approach. *Sci. Rep.* **2025**, *15*, 39846. [CrossRef] [PubMed]
55. Hou, W.; Li, X.; Yang, L.; Ta, W.; Jia, X. Carrying Capacity of Water Resources for Renewable Energy Development in Arid Regions in Northwest China: A Case Study of Golmud, Qinghai. *Front. Environ. Sci.* **2022**, *10*, 892414. [CrossRef]
56. Liu, W.; Wang, Y.; Huang, J.; Zhu, W. Assessment on the sustainability of water resources utilization in Central Asia based on water resources carrying capacity. *J. Geogr. Sci.* **2023**, *33*, 1967–1988. [CrossRef]

Disclaimer/Publisher's Note: The statements, opinions and data contained in all publications are solely those of the individual author(s) and contributor(s) and not of MDPI and/or the editor(s). MDPI and/or the editor(s) disclaim responsibility for any injury to people or property resulting from any ideas, methods, instructions or products referred to in the content.